European Journal of Pharmaceutical Sciences 213 (2025) 107225

Contents lists available at ScienceDirect

European Journal of Pharmaceutical Sciences

journal homepage: www.elsevier.com/locate/ejps

Bioinspired mycobacterial lipid coating of porous particles for enhanced antimicrobial efficacy

Jesús E. Campos Pacheco [a,b,*], Camilla Davids [c], Tetiana Yalovenko [a,b], Elin Nässtrom [d], Maria Ahnlund [d], Gabriela Godaly [c], Sabrina Valetti [a,b,*]

[a] Biomedical Science, Faculty of Health and Society, Malmö University, 20506 Malmö, Sweden
[b] Biofilms – Research Centre for Biointerfaces (BRCB), Malmö University, 20506, Malmö, Sweden
[c] Department of Microbiology, Immunology and Glycobiology, Institution of Laboratory Medicine, Lund University, 223 62 Lund, Sweden
[d] Swedish Metabolomics Centre, Umeå Plant Science Centre (UPSC), Department of Forest Genetics and Plant Physiology, Swedish University of Agricultural Sciences, 901 83, Umeå, Sweden

ARTICLE INFO

Keywords:
Mycobacterium bovis BCG
Bacterial lipids
Clofazimine (CLZ)
Mesoporous silica particles (MSPs)
Lipid coating
Cardiolipin
Mycobacterial infections

ABSTRACT

The study aimed to investigate the unique lipid composition of Mycobacterium bovis BCG and its potential to enhance antimicrobial efficacy of lipid-coated mesoporous silica particles (MSPs). The bacterial lipids (BL) were extracted with petroleum ether and analyzed via LC-MS, revealing a complex mixture of phospholipids, including cardiolipin, phosphatidylcholine, phosphatidylethanolamine, and triacylglycerols. Lipid coating (using bacterial lipids and lung surfactant DPPC as the main component) was performed on MSPs via vesicle fusion approach and confirmed with ATR-FTIR spectroscopy. MSPs were loaded with clofazimine (CLZ), as a drug model for tuberculosis. The obtained BL-DPPC-coated CLZ-MSPs were more effective in inhibiting mycobacterial growth and killing intracellular mycobacteria compared to uncoated and DPPC-coated CLZ-MSPs. The bacterial lipids showed a good safety profile on M1-like and M2-like human primary macrophages without inducing a strong immune response or formation of foam cells. These findings suggest that the obtained bacterial lipid coatings can improve antimicrobial efficacy in treating both extracellular and intracellular mycobacteria infections directly in the lungs.

1. Introduction

Tuberculosis (TB) is one of the top ten causes of death worldwide. It is estimated that TB kills 3425 people every day and about one-quarter of the world's population is infected. In 2023, an estimated 10.8 million people fell ill with TB, including 1.3 million children (WHO 2025; Migliori et al., 2025). According to WHO, there were 558 000 new cases with resistance to rifampicin– the most effective first-line drug, of which about 82 % had multidrug-resistant. One of the targets of the UN Sustainable Development Goals is to end the global TB epidemic by 2030. Considering the elevate TB incidence together with the spread of antibiotic-resistant microorganisms, TB is a huge threat to the world society that urge immediate actions. The treatment of TB comprises the association of several antibiotics (up to seven in case of multi-drug resistance) with distinct mechanism of action in order to target different bacterial signaling pathways and induce synergistic effects that allows reducing each single drug dose and decreasing the side effects (WHO 2025; Seung et al., 2015; Matteelli et al., 2025). However, different in vivo pharmacokinetic profiles that make the drugs arriving at the infected site at different time affect the understanding of the synergistic antimicrobial effect. Other challenges in TB treatment include reaching the intracellular residing bacteria in the airways and in the granuloma, and addressing multidrug-resistant strains.

Inhalation therapies are highly recommended for early infections and acute late-stage cases when most bacteria are located in the lungs. Despite various studies of different drug carriers (e.g., lactose, mannitol spray dried particles) have been investigated for inhalation therapy very few have advanced to new products. Mesoporous silica particles (MSPs) are biocompatible carriers composed by amorphous silicon dioxide (SiO_2) organized as solid particles that contains thousands of pores within the "*meso*" range (i.e. 2 - 50 nm) offering vast surface area and large pore volumes (up to 1300 m^2/g and 1.5 cm^3/g) and allowing high cargo loading (up to 50 % w/w of drug content) (Mamaeva et al., 2013). MSPs can be synthesized as spherical free flowing particles suitable for

* Correspondence author.
E-mail addresses: jecp.usb@gmail.com (J.E. Campos Pacheco), sabrina.valetti@mau.se (S. Valetti).

https://doi.org/10.1016/j.ejps.2025.107225
Received 3 April 2025; Received in revised form 19 July 2025; Accepted 4 August 2025
Available online 6 August 2025

dry powder inhalation (with an aerodynamic diameter between 1 and 5 μm). In this context, our research group has demonstrated the potential of MSPs as the sole excipient for dry powder inhalation formulation, offering a novel and versatile strategy for drug delivery to the lungs of protein (Rocío Hernández et al., 2024) and the antitubercular drug clofazimine (CLZ) in treating TB infections (Campos Pacheco et al., 2024; Campos Pacheco et al., 2025). These micron-sized spherical particles had an excellent aerodynamic profile, dissolved in lung fluid and generated nanoparticles. This dual micro-nano inhalation approach enhanced both extracellular and intracellular drug delivery. Taking inspiration from nature and the main phospholipid components of the lung surfactant (i.e., DPPC), DPPC-coated MSPs showed a marked improvement of CLZ dissolution rate while enhancing the interaction with lung surfactant, mucus and lung epithelial tissue. This study investigated the impact of phospholipids and bacterial lipid coatings on the antimycobacterial activity of CLZ-encapsulated MSPs against mycobacteria (Campos Pacheco et al., 2025).

Lipid-based delivery systems derived from the bacterial membrane have emerged as promising platforms for both vaccine and drug delivery applications. For example, lipid reconstituted nanoparticles (LrNs) and PLGA-LrNs formulated from *Mycobacterium smegmatis* membrane extracts have demonstrated improved stability and synergistic antibacterial activity when loaded with plant-derived antimicrobials against this surrogate model organism (Pu et al., 2024). Similarly, liposomes constituted with membrane lipids from *Mycobacterium smegmatis* have been shown to localize within the same endosomal compartments as the pathogen and to enhance both drug retention and proinflammatory signaling, leading to more effective intracellular pathogen eradication (Mishra et al., 2023).

In this context, the aim of this study was to explore the unique lipid composition of *Mycobacterium bovis* BCG and its potential to enhance the antimicrobial efficacy of lipid-coated MSPs, while maintaining the main lung lipid surfactant, DPPC, as major lipid component. Additionally, the study aimed to understand the effects of bacterial lipid coated MSPs on human primary macrophages and dTHP-1 cells, particularly in terms of mitochondrial activity and cell morphological changes.

2. Materials and methods

2.1. Materials

Mesoporous Silica Particles (MSPs) were provided from Nanologica AB (Södertalje, Sweden), batch EA1791 (SPIRO). 1,2-dipalmitoyl-sn-glycerol-3-phosphocholine (16:0 PC, DPPC) was purchased from Avanti® (VWR, Stockholm, Sweden). Clofazimine (CLZ) was purchased from Chemtronica A.B. (Sollentuna, Sweden). Phosphate Buffer Saline (PBS) tablets were supplied from Sigma-Aldrich (Tyreso, Sweden), and calcium chloride dihydrate was supplied from Merck (Solna, Sweden. Ethanol (analytical grade) was supplied from Solveco (Rosersberg, Sweden) and acetone was supplied from VWR (Stockholm, Sweden). For experiments with macrophages, RPMI medium 1640 (ATCC modification), FBS, penicillin/streptomycin solution, phosphate buffered saline (PBS), granulocyte-macrophage colony stimulating factor (GM-CSF), macrophage colony stimulating factor (M-CSF) and Accutase were all purchased from Gibco™, Fisher Scientific GTF AB (Gothenburg, Sweden). Phorbol 12-myristate 13-acetate (PMA) and 2-(3,5-diphenyltetrazol-2-ium-2-yl)-4,5-dimethyl-1,3-thiazole; bromide (MTT) were purchased from Fisher Scientific GTF AB (Gothenburg, Sweden). 7-AAD and Oxidized Low-density Lipoprotein (ox-LDL) from Invitrogen™, Fisher Scientific GTF AB (Gothenburg, Sweden). Human TNF-α, Human IL-10, Human CCL2/MCP-1, DuoSet ELISA were purchased from Bio-Techne Ireland Limited (Dublin, Ireland). Dimethyl sulfoxide (DMSO) was purchased from Fisher BioReagents™, Fisher Scientific GTF AB (Gothenburg, Sweden). Ficoll-Paque PLUS was purchased from GE Healthcare (Uppsala, Sweden). Monocyte Attachment Medium (MAM) was from PromoCell, Mediqip (Älvsjö, Sweden). Antibodies CD80-APC (Clone REA661) and CD206-PE (Clone DSN228) were purchased from Miltenyi Biotec Norden AB (Lund, Sweden). Formalin 10 %, Q Path®, buffered was from VWR Q-Path Chemicals. Isopropanol min. 99.5 % was purchased from Histolab Products AB (Askim, Sweden).

For the LC-MS analysis, methanol and acetonitrile, HPLC-grade, were obtained from Fischer Scientific (Waltham, MA, USA), 2-Propanol, HPLC-grade was obtained from VWR (Radnor, PA, USA), Chloroform, Suprasolv for GC was obtained from Merck (Darmstadt, Germany), H_2O (Milli-Q), and Ammonium formate was obtained from Sigma (St. Louis, MO, USA). Reference and tuning standards: Purine, 4 μM, Agilent Technologies (Santa Clara, CA, USA) HP-0921 (Hexakis(1H, 1H, 3H-tetrafluoropropoxy)phosphazine), 1 μM, Agilent Technologies (Santa Clara, CA, USA) Calibrant, ESI-TOF, ESI-L Low Concentration Tuning Mix, Agilent Technologies (Santa Clara, CA, USA) HP-0321 (Hexamethoxyphosphazine), 0.1 mM, Agilent Technologies (Santa Clara, CA, USA).

2.2. Nanoconfinement of drug molecules inside the internal porosity of mesoporous silica particles

The mesoporous silica particles (MSPs) were synthesized by Nanologica AB (publ.) by their proprietary method followed a sol-gel synthesis (Chunfang Zhou and Paszkiewicz, 2018) and clofazimine (CLZ) was loaded in MSPs as showed in on our previous work (Campos Pacheco et al., 2024). Briefly, CLZ was dissolved in acetone (2 mg/mL) and the MSPs suspended in this solution (20 mg/mL). This mixture was stirred gently for 2 h using a rotavapor. The solvent was evaporated at 40 °C and under reduced pressure (250 mbar), and the vacuum system was maintained for 2 h. The formulation (i.e., CLZ-MSPs) was placed in the fume hood to dry completely during 24 h.

2.3. Lipid extraction

Mycobacterium bovis bacillus Calmette-Guerin (BCG) belongs to the *M. tuberculosis* complex which makes them closely related to *M. tuberculosis*, the bacterium that causes tuberculosis (TB). The BCG were grown in Middlebrook 7H9 broth, supplemented with supplemented with 0.05 % Tween 80, 0.2 % glycerol and 10 % ADC enrichment (Middlebrook Albumin Dextrose Catalase Supplement, Becton Dickinson, Oxford, UK) as described previously (Rao et al., 2021). The bacterial culture was washed twice with sterile PBS (10 min centrifugation at 3000 × *g*), re-suspended in broth, and then dispensed into vials. Glycerol was added to a final concentration of 25 % and the vials were frozen at −80 °C. Prior to each experiment, a vial was defrosted, added to 9 ml of 7H9/ADC medium, and incubated with shaking for 72 h at 37 °C. The mycobacteria was then centrifuged for 10 min at 3000 × *g*, washed twice with PBS, and re-suspended in 10 mL of PBS.

BCG was heat-inactivated at 80 °C for 20 min before being stored at −20 °C in the freezer.

Extraction method 1: The extraction method 1 followed an already reported protocol in literature (Ferreras et al., 2008). 5 mL of inactivated BCG was resuspended with 35 mL of MeOH:NaCl 0.3 % w/v 9:1. 40 mL of petroleum ether (PE) was added and mixed gently in a funnel separator. The layer of PE is up and the aqueous below after 24 h separation and equilibrium. The organic phase was stored and the aqueous phase was extracted again with 40 mL PE. And this process was repeated once more. The organic fractions were filtered using a pre-burnt glass filter and concentrated using rotavapor at 50–60 °C., 250 mbar. The concentrated solution was eventually placed in a vial and the solvent was evaporated by N_2 flow and afterwards 24 h under vacuum in desiccator. This extraction process was conducted on two different batches of BCG, cultivated in different times.

Extraction method 2: The extraction method 2 followed an already reported protocol in literature (Boiten et al., 2016). Using a modified Bligh and Dyer method, 2.5 mL of heat killed BCG was suspended in 15 mL of $CHCl_3$:MeOH (1:2 v/v). The suspension was stirred for 2 h at 40 °C

to extract as much lipid as possible. The suspension was concentrated to 1 mL and stored at 4 °C. The non-soluble mixture was resuspended in 15 mL $CHCl_3$:MeOH (1:1 v/v). The suspension was stirred for 2 h under same conditions, concentrated into 1 mL and resuspended with 15 mL $CHCl_3$:MeOH (2:1 v/v), finalizing with more organic solvent during the stirring and extraction for 2 h. The process of extracting with $CHCl_3$: MeOH 1:2, 1:2 and 2:1 and concentration into 1 mL was repeated same conditions. And the final concentrated solid was suspended in 40 mL $CHCl_3$ 100 %, and this volume was fractioned with 40 mL of 10 mM KCl. After 24 h separation in a separator funnel, the organic phase was filtered using a pre-burnt glass filter. The solvents were evaporated by rotavapor and N_2 flow and afterwards stored 24 h under vacuum in desiccator.

2.4. Lipid analysis

Lipid profiling by LC-MS was performed at the Swedish Metabolomics Center in Umeå, Sweden according to Diab et al. (2019) with some modifications (Diab et al., 2019). Dry lipid extract sample was dissolved in 2:1 v/v $CHCl_3$:MeOH to a concentration of 300 ng/μL.

2.4.1. LC-MS analysis

The chromatographic separation was performed on an Agilent 1290 Infinity UHPLC-system (Agilent Technologies, Waldbronn, Germany). 1 μL of each sample were injected onto an Acquity UPLC CSH, 2.1 × 50 mm, 1.7 μm C18 column in combination with a 2.1 mm x 5 mm, 1.7 μm VanGuard precolumn (Waters Corporation, Milford, MA, USA) held at 60 °C. The gradient elution buffers were A (60:40 acetonitrile:water, 10 mM ammonium formate, 0.1 % formic acid) and B (89.1:10.5:0.4 2-propanol:acetonitrile:water, 10 mM ammonium formate, 0.1 % formic acid), and the flow-rate was 0.5 mL min-1. The compounds were eluted with a linear gradient using initial condition 15 % B, and increase to 30 % B at 1.2 min, 55 % at 1.5 min, isocratic to 5 min, increase to 72 % B at 7 min, 85 % at 9.5 min and 100 % B at 10 min, and then held at 100 % for 2 min. An additional wash of the injection valve, with 100 % B and flowrate 5.0 mL min-1 for 0.3 min, was performed before decreased to initial condition 15 % B over 0.3 min; these conditions were held for 1.1 min to equilibrate the column before next injection. The compounds were detected with an Agilent 6546 Q-TOF mass spectrometer equipped with a jet stream electrospray ion source operating in positive ion mode. A reference interface was connected for accurate mass measurements; the reference ions purine (4 μM) and HP-0921 (Hexakis(1H, 1H, 3H-tetrafluoropropoxy)phosphazine) (1 μM) were infused directly into the MS at a flow rate of 0.05 mL min-1 for internal calibration, and the monitored ions were purine *m/z* 121.05 and HP-0921 m/z 922.0098. The gas temperature was set to 150 °C, the drying gas flow to 8 L/min and the nebulizer pressure 35 psig. The sheath gas temp was set to 350 °C and the sheath gas flow 11 L/min. The capillary voltage was set to 4000 V in positive ion mode. The nozzle voltage was 300 V. The fragmentor voltage was 120 V, the skimmer 65 V and the OCT 1 RF Vpp 750 V. The collision energy was set to 0 V. The *m/z* range was 100 - 2600, and data was collected in centroid mode with an acquisition rate of 6 scans s^{-1}. Automated iterative MSMS was performed in three stages. The collision energies were set to 25 and 40 eV. The acquisition rate was 3 scans s^{-1}. Static exclusion was set at a range of 100–800 m/z.

Data analysis-evaluation/statistical methods

All data processing was performed using the Agilent MassHunter Profinder version B.10.0.2 (Agilent Technologies Inc., Santa Clara, CA, USA). For target processing, a pre-defined list of lipids was searched for using the Batch Targeted feature extraction in MassHunter Profinder. An in-house LC-MS library built up by authentic standards run on the same system with the same chromatographic and mass spectrometry settings, was used for the targeted processing. The identification of the lipids was based on MS, MSMS fragments, and retention time information. The detected lipid species were from the following lipid classes: cardiolipin (CL), phosphatidylcholine (PC), phosphatidylethanolamine (PE) and triacylglycerol (TG). Results were expressed as area under the curve (AUC) values from the extracted ion chromatograms of each lipid molecule.

2.5. Lipid coating of loaded and unloaded MSPs by vesicle fusion

Our previous study and optimized method was followed for the preparation of lipid coated MSPs for inhalation via vesicle fusion (Campos Pacheco et al., 2025). DPPC was chosen as main phospholipid since they are part of the main lung surfactant (Wauthoz and Amighi, 2014) and the demonstrated mucoadhesive and mucus-penetrating behaviour (Campos Pacheco et al., 2025). The bacterial lipid extracted with method 1 were mixed in proportion of 0.5 w/w or 20 % w/w with DPPC. Briefly, 20 mg of lipids (DPPC or BL-DPPC) was dissolved with chloroform (1 mL). A lipid film was prepared by evaporating the solvent under nitrogen flow and maintained under vacuum overnight. Then the lipid film was rehydrated at 10 mg/mL in PBS (10 mM phosphate buffer, 2.7 mM KCl, 137 mM NaCl, pH 7.4 at 25 °C) and put in a water sonication bath for 5 min at 55 °C to produce liposomes. The suspension was further dispersed with an ultrasonication probe (Branson Ultrasonics, Brookfield, USA), at a 400 W power, 20 % amplitude and pulse duration of 0.5 s (intermittent) for 10 min to reduce size and lamellarity of liposomes. An aqueous solution of 8 mM $CaCl_2$ was added in a 1:1 ratio to the liposome's suspension. The final concentration of liposomes was 5 mg/mL in 5 mM PBS with 4 mM $CaCl_2$. Dynamic Light Scattering (DLS) (Zetasizer Ultra, Malvern Panalytical) was used for investigating the particle size of vesicles. Vesicles dispersed in PBS were diluted 1:10 with milli-Q Water and 1 mL was transferred in a single-use cuvette (VWR, Radnor, USA). The particle size was measured by MADLS (Multi Angle Dynamic Light Scattering), which considers angles of 173° (back scatter), 90° (side scatter), and 13° (forward scatter) The refractive index was adjusted directly with the pre-established method of DLS for liposomes. And the temperature was set at 25 °C with equilibration time of 120 s prior to analysis (triplicate).

MSPs or CLZ-MSPs (5 mg/mL) was suspended in PBS (5 mM), mixed using vortex and sonicated for 5 min. To form the lipid coated-MSPs, the resulting liposomes were added (drop by drop) to the suspension of MSPs under bath sonication for 5 min at 50 °C at a ratio of 1:5 lipids/MSPs. This temperature supposed to be higher than the lipid melting point for DPPC and most lipids expected to be in the mixture, as showed by differential scanning calorimetry. Particles were then centrifuged at 1500 × *g* for 10 min and unbound liposomes were removed with the supernatant. Resulting DPPC or BL-DPPC-coated MSPs were rinsed by resuspending in 2 mL PBS and later with 2 mL of milli-Q Water, centrifuging at 1500 × *g* for 10 min, with subsequent removal of supernatant each time. MSPs were rinsed twice in PBS while CLZ-MSPs once. Finally, the particles were dried with a centrifugal evaporator SP Genevac miVac (Warminster, United Kingdom) equipped with a condenser (SpeedTrapcou), at 40 °C overnight. The samples were stored in the freezer at −20 °C up to 1 month.

2.6. Characterization of dry powder formulation

2.6.1. ATR-FTIR

The lipid coated- silica and lipid coated- drug loaded samples were characterized with a Thermo Nicolet 6400 spectrometer (Thermo Fisher, Waltham, USA) equipped with a liquid-nitrogen-cooled MCT-A detector (Thermo Fisher, Waltham, USA). A Smart iTR accessory (Thermo Fisher, Waltham, USA) was used to obtain ATR-FTIR spectra. 100 scans were conducted for each ATR-FTIR spectrum at a resolution of 8 cm^{-1} in the wavenumber range of 4000–400 cm^{-1}. To calibrate ambient air and absorbance of the diamond, a new background was acquired prior to each new spectrum collection.

2.6.2. Drug quantification in dry powder formulation for inhalation

10 mg of formulations (triplicates of CLZ-MPS and DPPC coated-

CLZ-MSPs) were mixed with methanol (0.2 mg/mL) and placed under sonication to release of CLZ from MSPs. The mixture was centrifugated at 3000 × *g* for 15 min. The supernatant was extracted and diluted 10 times with MeOH. The samples were filtered with 13 mm, 0.2 μm PTFE filters and then analysed with HPLC. HPLC analysis was performed with an Agilent 1100 HPLC system, equipped with a binary gradient pump with degasser (G1322A), autosampler (G1316A), thermostated column compartment (G1315A) and a diode array UV/ visible detector (G1362B). All data collection was performed using the OpenLAB CDS program. For the drug analysis, a suitable isocratic method was developed using a 4.6 × 150 mm column, 3.5 μm (SVEA® C18 column, Nanologica AB (publ), Södertälje, Sweden). Mobile phase A consisted of HPLC milliQ-water quality water with 0.05 % v/v trifluoroacetic acid (TFA). Mobile phase B was acetonitrile. A flow rate of 0.8 mL/min was used for all measurements. Mobile phases A and B were mixed in a 40:60 ratio by the pump. The column temperature was 40 °C. A detection wavelength of 286 nm and the injection volume of 50 μL was used. Calibration curve of CLZ were prepared in a concentration range of 0.15 – 5 μg/ml in pure MeOH since it is the solvent for drug content analysis. CLZ retention time was around 4 min. The collection time per analysis was 7 min. The detection wavelength was 286 nm and the injection volume 5 μL. The obtained calibration curve had a $R^2 = 0.9974$ The limit of detection (LOD) and quantitation (LOQ) for the drug quantification methods were 39.4 and 13.1 ng/mL, respectively.

2.6.3. Differential scanning calorimetry (DSC)

DSC was used to determine the phase transition of DPPC and BL-DPPC (with 20 % BL w/w). A DSC STAR^e System (METTLER TOLEDO) was used. Lipid-coated MSPs samples (2–3 mg) were loaded in an aluminium pan and placed in the instrument for analysis with a heating-cooling program from 25 to 250 °C and then from 250 to 25 °C at a rate of 10 °C min^{-1}. The nitrogen flow rate was 40 mL/min. To calibrate and set up the temperature scale and enthalpy measurement, an empty pan was used.

2.7. Cell culture studies

2.7.1. Cell culture

Human venous blood mononuclear cells were obtained from healthy volunteers using a Lymphoprep density gradient (Axis-Shield, Oslo, Norway) as described previously (Tenland et al., 2018). To obtain pure monocytes, CD14 micro beads were applied to the cell suspension, washed and passed through a LS-column according to manufacturer's description (130–050–201, 130–042–401, Miltenyi Biotec, USA).

For infection experiments, the monocytes were counted (Sysmex), diluted in RPMI 1640 supplemented with 5 % FCS, NEAA, 1 mM Sodium Pyruvate, 0.1 mg/ml Gentamicin (11,140–035, 111,360–039, 15,710–49, Gibco, Life Technologies) and 50 ng/ml GM-CSF (215-GM, R&D systems) and seeded in 96-well plates (105/well) for a week to differentiate into macrophages. Infection experiments were performed in RPMI 1640 without Gentamicin.

THP-1 (TIB-202) is a monocyte cell line isolated from peripheral blood from an acute monocytic leukemia patient was purchased from American Type Culture Collection (ATCC, Manassas, VA, USA) and grown at 37 °C and 5 % CO_2. The ATCC guidelines for thawing and maintaining cells were strictly adhered to. The cell culture medium used was RPMI 1640 (ATCC modification), supplemented with 20 % heat-inactivated FBS for the first three passages after thawing and 10 % FBS for all subsequent passages. Additionally, the medium included 1 % penicillin/streptomycin (10,000 units/mL of penicillin and 10,000 μg/mL of streptomycin). The medium was refreshed every 3–4 days, and cells were passaged every 7 days. To induce the differentiation of THP-1 cells into macrophage-like cells, 4×10^4 cells per well were seeded in 96-well plates (Sarstedt, Cell+, Flat Base, Yellow, Germany) and incubated at 37 °C with culture media supplemented with 50 ng/mL PMA for 48 h. After this period, the cells were thoroughly washed with 200 μL of pre-warmed (37 °C) PBS per well to obtain adherent PMA-differentiated THP-1 cells (dTHP-1).

2.7.2. Foam cell formation assay

The dTHP-1 cells were prepared in the 96-well plates as described above. Cells were incubated with 100 μL/well of tested samples (BL, DPPC-MSPs, BL-DPPC-MSPs, MSPs) for 24 h. The particles concentration was 0.06 mg/mL, as identified as safe concentration in our previous study (T. Yalovenko et al.), and the bacterial lipid was 0.01 μg/mL in the serum free RPMI medium, ensuring an excess compared to the amount present on the particle surface. The serum free RPMI medium was used as a negative control. 100 μg/mL ox-LDL was used as a positive control. After the treatment, the cells were washed with PBS (the same volume as a treatment) and fixed with 10 % formalin for 30 min at room temperature. THP-1 cells were then stained with Oil Red O for 20 min at room temperature in dark place followed by very quickly rinsing with 60 % isopropanol to remove excess stain and gently washed 2 times with PBS to remove any residual isopropanol. Cells were examined in PBS by light microscopy (×20 and ×40).

2.7.3. Bacterial lipids effect on mitochondrial activity and cell morphology

To differentiated into classically activated M1 and alternatively activated M2 macrophages, 50 ng/mL of GM-CSF for M1 differentiation or 50 ng/mL of M-CSF for M2 differentiation were used on isolated PBMCs (see section above). After three days of incubation at 37 °C and 5 % CO2, 1 mL of cell culture medium was carefully removed from the top layer of each well. The wells were then supplemented with 1 mL of fresh medium containing double the concentration (100 ng/mL) of GM-CSF or M-CSF, depending on the differentiation required, and incubated for an additional three days. To evaluate the phenotype after THP-1 differentiation and human primary macrophage polarization, the surface markers CD80 and CD206 were measured via flow cytometry. Cells (2×10^5) were transferred to flow cytometry tubes and centrifuged at 300 × *g* for 5 min. Cells were resuspended in PBS containing 0.5 % FBS and stained with APC-labeled anti-CD80 and PE-labeled anti-CD206 (Miltenyi Biotec Norden AB, Lund, Sweden), along with appropriately labelled isotype controls. Cell viability was assessed by staining with 7-AAD (Invitrogen™, Fisher Scientific GTF AB, Gothenburg, Sweden). The samples were analyzed via flow cytometry (BD Accuri™ C6 Plus, Biosciences, Le Pont de Claix, France) and BD Accuri C6 Plus Software, version 1.0.34.1. The mean fluorescence intensities were collected between 585 and 540 nm for the PE fluorochrome, 670 nm longpass (LP) filter for the 7-AAD fluorochrome, and 675–625 nm longpass (LP) filter for the APC fluorochrome, with the 488 nm line of an argon laser used for excitation. A total of 10,000 events were collected at the defined gates. Data are presented in Fig. S7, supplementary information.

The mitochondrial activity of M1 and M2 macrophage cells after incubation with bacterial lipids was investigated by MTT test. Cells were incubated in 96-well plates (10,000 cells/well) with bacterial lipids (0.5 mg/mL) at 37 °C and 5 % CO_2. Negative control (untreated samples) was prepared by incubating the cells with the same medium and conditions without lipids. After 24, cells were thoroughly washed with 200 μL of pre-warmed (37 °C) PBS per well to remove any residual media. Next, 90 μL of fresh PBS and 10 μL of a 5 mg/mL MTT reagent solution in PBS were added to each well. The blank wells, which was reserved for absorbance interference control, did not receive the MTT reagent. After a 2.5-hour incubation, the MTT solution was carefully removed, and 100 μL of DMSO was added to solubilize the formazan crystals. For the blank wells, 100 μL of PBS was added instead of DMSO. The plates were placed on a gentle shaker for 10 min to ensure thorough homogenization while being protected from light. Absorbance was measured at 570 nm using a Tecan Safire microplate reader (Florida, USA) and accounted for by subtracting the absorbance of the blank well. The percentage of mitochondrial activity was calculated as the ratio of absorbance of treated cells to that of untreated cells.

2.7.4. Cytokine analysis

BL-DPPC—CLZ-MSPs were incubated with primary human macrophages for 24 h at 37 °C, 5 % CO_2 at a concentration range between 0.1563 ng/mL - 10 ng/mL. Rifampicin (1 ng/mL) was used as a control. Supernatants were aspirated and analysed for cytokines TNFα and CCL2 (R&D Systems, DTA00D, DY279–05) using the fluorescence intensity.

For CCL2, a 96-well microplate was coated with Mouse Anti-human MCP-1 capture antibody (1 μg/mL) and incubated overnight at room temperature. After three washes with 1X Wash Buffer, Reagent Diluent was added to block non-specific binding, followed by a 1-h incubation at room temperature. The plate was washed again, and the collected supernatants, along with Human MCP-1 standards, were added and incubated for 2 h at room temperature. Following another wash, Biotinylated Goat Anti-human MCP-1 detection antibody (25 ng/mL) was added and incubated for 2 h. After washing, Streptavidin-HRP (1:40) was added and incubated for 20 min in the dark. The plate was washed once more, substrate solution was added, and the plate was incubated for another 20 min in the dark. The reaction was stopped with Stop Solution, and absorbance was measured at 450 nm using a Tecan Infinite F200 microplate reader.

For TNF-α, the supernatants, Human TNF-α standards, and Assay Diluent RD1F were added to a pre-coated Human TNF-α microplate. The plate was incubated on a horizontal orbital shaker (450 rpm) at room temperature for 2 h, then washed three times with 1X Wash Buffer. Human TNF-α conjugate was added, followed by another 2-h incubation under the same conditions. After washing, substrate solution (Color Reagents A and B) was added and incubated for 30 min in the dark. The reaction was stopped with Stop Solution, and absorbance was measured at 450 nm using a Tecan Infinite F200 microplate reader.

2.8. Antimicrobial activity

2.8.1. Minimum inhibitory concentration (MIC)

The resazurin microtiter assay (REMA) was used to determine the minimum inhibitory concentration (MIC_{99}) as reported previously (Tenland et al., 2019). Nanoparticles containing CLZ (10 μL) was added to bacterial suspensions (90 μL) on a 96-well plate at a concentration range between 0.0001563 mg/mL −0.01 mg/mL. A negative control and a positive control were diluted from OD 0.01 to 1/10 and 1/100 were included onto the plate and incubated at 37 °C, 5 % CO_2. Extra controls were untreated bacteria and rifampicin (0.001 mg/mL) treated mycobacteria. MIC was determined by the color change using resazurin (1:10 v/v, PrestoBlue Cell viability reagent, Thermo Scientific). MIC was determined after one week for most strains by adding 10 μl resazurin followed by incubation overnight, corresponding to 99 % inhibition.

2.8.2. Intracellular killing

Infection of primary human macrophages was done with a modified protocol from previously described methods (Tenland et al., 2018). Briefly, macrophages and BCG were mixed in a tube at a multiplicity of infection (MOI) of 10:1 and seeded and incubated for 24 h at 37 °C, 5 % CO_2. Extracellular bacteria was killed by adding amikacin to the media and incubating the cells for 30 min at 37 °C, 5 % CO_2. The attached cells were washed three times with PBS, resuspended with DMEF-12/HEPES/FCS, and treated with the compounds at a concentration range between 0.1563 ng/ml - 10 ng/ml. The cells were then incubated at 37 °C, 5 % CO_2 for one week. To determine the intracellular killing capacity, the cells were lysed with sterile water for 30 min and incubated with Presto blue cell reagent (Thermofisher) for 24 h at 37 °C, 5 % CO_2. The following day the fluorescence intensity was measured at 620 nm.

2.8.3. Human serum stability assay

BL-DPPC—CLZ-MSPs were incubated in human serum at a concentrations range of 0.156 to 10 ng/mL for 1, 2 and 3 h at 37 °C, 5 % CO_2 according to the previously described protocol (Tenland et al., 2019). The serum was used to prepare the serial dilutions of the compound. After each time point, 10 μl of serum-incubated BL-DPPC—CLZ-MSPs was added to 90 μl of BCG suspension and incubated at 37 °C, 5 % CO_2 for 4 to 7 days. Prestoblue was added to the cells and incubated overnight at 37 °C, 5 % CO_2. The following day the fluorescence intensity was measured at 620 nm.

2.8.4. Ethical statement

Blood for monocyte isolation and serum analysis was donated by healthy volunteers (Local Ethical Review Board approvals Dnr 2011/403 and 2014/35). All volunteers received both verbal and written information regarding the study's purpose, duration, and potential risks and benefits. No personal data were collected, and the blood samples were pooled.

3. Results

3.1. Characterization of the extracted bacterial lipid

The aim of extracting lipids from BCG was to explore the unique lipid composition of this bacteria, which is used as a vaccine against tuberculosis (Hiraishi et al., 2011), as bioinspired coating of drug delivery carrier. Therefore, bacterial lipids (BL) have been explored here as potential strategy to coat MSPs to deliver a poorly soluble drug such as clofazimine (CLZ). Thereby, the investigation addresses unmet needs to improve the killing efficacy of the drug against pulmonary and extrapulmonary TB. Understanding the lipid profile of BCG can provide insights into its immunogenic properties and how it interacts with the host immune system. To further elucidate the role of the lipids extracted from BCG, a crucial aspect is to analyze the lipid composition and therefore correlate the type of lipids with its effect in healthy and infected macrophages. Initial untargeted lipid analysis did not reveal significant differences in the lipid profiles obtained with extraction method 1 and 2; therefore, method 1 was selected for the remainder of the investigation. Fig. 1 presents the lipidomics of the petroleum ether extract isolated from the BCG pellet (method 1). The Total Ion Chromatogram (TIC) in Fig. 1A shows the variety and complexity of the lipid mixture. Polar lipids such as phosphatidylcholine (PC) and phosphatidylethanolamine (PE) were identified in the mixture at 2.5 – 4 min, while cardiolipin (CL) and triacylglycerol (TG) were identified with significant peaks at 8.62 and 8.95 min, respectively. These last two classes of lipids were prominent since the extraction method with petroleum ether aimed to retrieve the apolar lipids. The pie chart further categorizes the lipid classes, providing a clear summary of the lipid composition. Table 1 summarized the number of lipids detected for these classes being TG the most abundant, followed by PC, CL and PE. Other important classes of lipids such as phosphatidylserine (PS), ceramide (CER) and sphingomyelin (SM) were not detected.

Among the classes of lipids detected, cardiolipin has been highlighted for its impact in modulating the immune response of macrophages (Reynolds et al., 2020). The MS spectrum in Fig. 1B confirms the presence of cardiolipin mass peak (1437 m/z). The subsequent fragmentation and MSMS analysis in Fig. 1C offer detailed insights into the molecular structure of the lipid. The zoom-in on key fragment ions is particularly valuable for understanding the fragmentation pattern. The schematic representation in Fig. 1D provides a visual summary of the cardiolipin structure, indicating major fragmentation sites and suggesting fatty acid lengths that match the observed fragments in the MSMS spectrum. This structural elucidation is crucial for accurate lipid identification and annotation, contributing to a deeper understanding of the lipid biochemistry.

With similar extraction methods, Pirson et al. (2012), identified other several apolar lipids, including trehalose dimycolate (TDM), trehalose monomycolate (TMM), phthiocerol dimycocersates (PDIMs), triacyl glycerol (TAG), pentacyl trehalose (PAT), phenolic glycolipid (PGL), and polar lipids like phosphatidylethanolamine (PE), that were

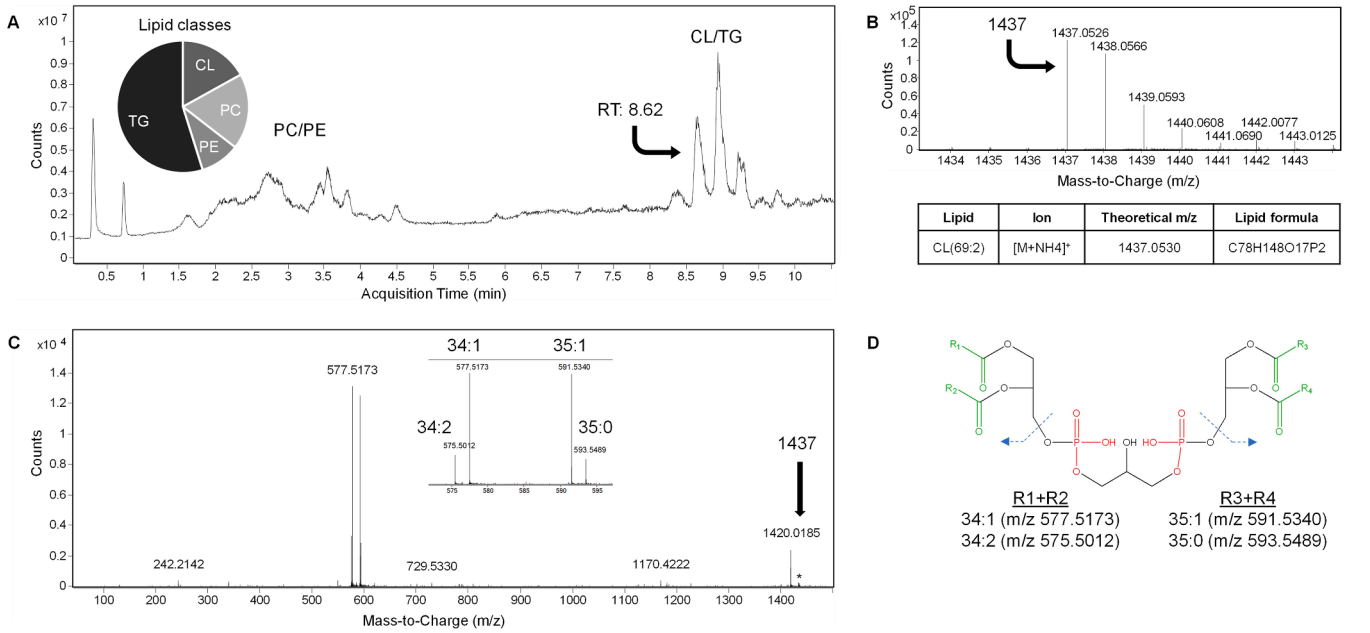

Fig. 1. Overview of lipid detection and annotation workflow. **A)** Total Ion Chromatogram (TIC) from lipid profiling of bacterial lipid with highlighted peak at 8.62 min, also including a pie chart with the different lipid classes detected, CL – cardiolipin, PC - phosphatidylcholine, PE - phosphatidylethanolamine, TG - triaclglycerol. **B)** MS spectrum of the highlighted peak corresponding to CL. **C)** The *m/z* is selected for fragmentation and fragments detected in MSMS spectrum, with zoom-in on interesting fragment ions. **D)** Schematic picture of a CL structure indicating major fragmentation sites together with suggested fatty acid lengths on each side (R1+R2 and R3+R4) matching the fragments in the MSMS spectrum.

Table 1
Summary of lipid classes searched for and detected in "bacterial lipid mixture".

Lipid	Found*	Lipid class
PE	12	Phosphatidylethanolamine
PS	ND	Phosphatidylserine
PI	ND	Phosphatidylinositol
PG	ND	Phosphatidylglycerol
PC	23	Phosphatidylcholine
Cer	ND	Ceramide
SM	ND	Sphingomyelin
DG	ND	Diacylglycerol
TG	68	Triacylglycerol
CL	21	Cardiolipin

* Number of lipids detected in each lipid class. ND – not detected.

not identified in our studies. Specifically, L. Quadri group has made important contributions to the characterization of apolar lipids from *M. tuberculosis, M. leprae, M. marinum* and *M. bovis.* with a particular focus on phenolic glycolipids (PGLs) and dimycocerosate esters (DIMs), associated with the virulence and pathogenesis of bacteria (Onwueme et al., 2005; Vergnolle et al., 2015). One limitation in these studies is that the composition of the lipids isolated can vary significantly between different strains. Therefore, future research exploring the lipidomic of various strains of the *M. tuberculosis* complex (e.g., *M. tuberculosis* or *M. bovis*) could provide a more comprehensive understanding of the lipid profiles and their biological roles.

3.2. Lipid coating of mesoporous silica particles

Overall, these data contribute to the lipidomic of BCG bacteria and open opportunities to explore therapeutic strategies, such as the coating of MSPs with the obtained bacterial lipids (BL) to increase efficacy against tuberculosis treatments. BL were coated onto MSP's surface using vesicle fusion approach, as we showed in a previous publication (Campos Pacheco et al., 2025). BL was mixed with DPPC, the phospholipid present in the lung surfactant, as 0.5 % w/w of BL and 99.5 % w/w of DPPC, while the ratio lipids:MSPs was fixed to 1:5 according to our previous optimizations (Campos Pacheco et al., 2025). ATR-FTIR spectroscopy was employed to characterize the lipid deposition on MSPs surfaces. Fig. 2 illustrates the ATR-FTIR spectra of lipid-coated particles, both with and without BL. The spectra reveal lipid deposition on both empty and clofazimine (CLZ) drug-loaded MSPs. CH_2 peaks (2858 cm^{-1} and 2927 cm^{-1}) and *C═O* (1727 cm^{-1}) indicate the presence of phospholipids (i.e., DPPC) (Jiang et al., 2005), which is similar to our previous study on phospholipid coating of MSPs (Campos Pacheco et al., 2025). The full FT-IR spectra is shown in Fig. S1 (supplementary information). The presence of CLZ after coating is confirmed by a prominent peak at 1564 cm^{-1}, attributed to N—H bending vibrations. This assignment aligns with previous studies using Nano-IR and conventional ATR-IR for analysing CLZ-MSPs (Campos Pacheco et al., 2024). Moreover, quantitative ATR-FTIR analysis (summarized in Table 2) using the C—H peaks of the spectra revealed that the DPPC deposited in DPPC—CLZ-MSP and BL-DPPC—CLZ-MSPs was (4.292 ± 0.037) % and (3.510 ± 0.004) %, respectively. The result suggests that the quantity of lipid deposited MSPs aligns well with our previous studies, and the presence of bacterial lipid (0.5 % of total lipid content) does not alter the DPPC deposition. Moreover, the content of CLZ in the dry powder formulations remained in the range of 3–4 % w/w (evaluated by HPLC).

Our results suggest that, at 0.5 % bacterial lipid (BL) content, the presence of BL does not markedly affect the success of vesicle fusion in coating mesoporous silica particles (MSPs)We hypothesized that is due to the regular formation of vesicles with high amount of DPPC (Table 1) in presence of bacterial lipids, which fused with silica surface. To support this, the vesicles size (Fig. S2, supplementary information) remains similar regardless the amount of bacterial lipids (i.e., 100 % DPPC, 99.5 % DPPC/0.5 % bacterial lipids, and 80 % DPPC/20 % bacterial lipids). Moreover, differential scanning calorimetry (DSC) indicates that the melting peak of the BL-DPPC mixture (20 % w/w BL) is similar to pure DPPC, suggesting that the primary phase transition temperature observed (Tm: 48.86 °C) for DPPC was not significantly altered by the presence of the bacterial lipid (Fig. S3, supplementary information). However, for the mixture sample some shoulders were observed in the

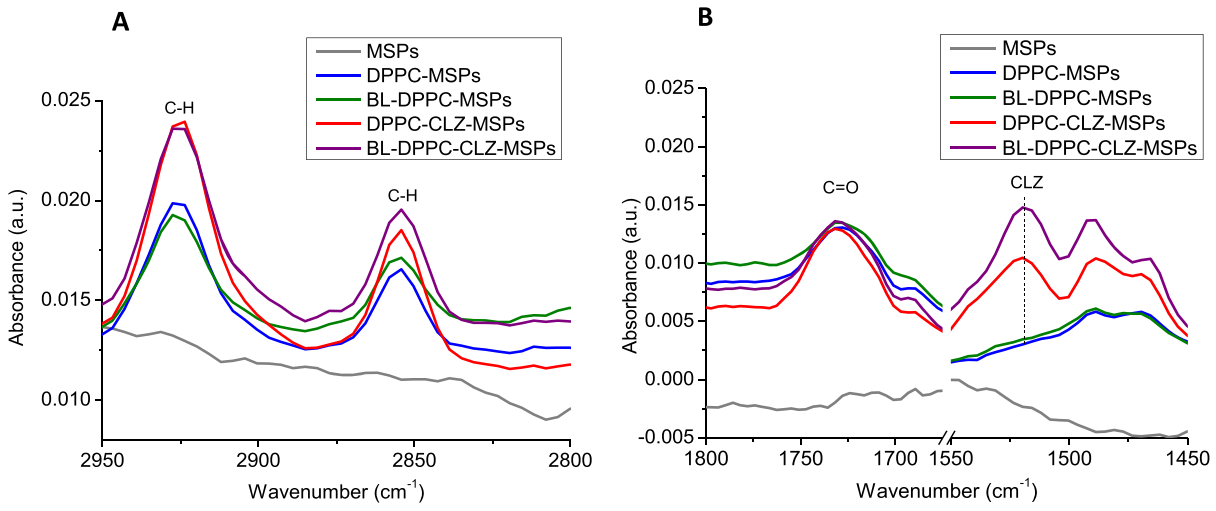

Fig. 2. ATR-FTIR spectra of the lipid coated MSPs: BL-DPPC—CLZ-MSPs, DPPC—CLZ-MSPs, unloaded and coated samples. **A)** Region of interest (2950 – 2800 cm^{-1}) for alkyl chain peaks. **B)** Region of interest (1800 – 1450 cm^{-1}) for carbonyl group and CLZ signal. The spectra are shown zoomed-in on different regions.

Table 2
Composition of the lipid-coated MSPs used in this study. DPPC content evaluated by ATR-FTIR (n = 2) and drug content evaluated by HPLC (n = 3). Values presented as average ± range.

	DPPC content (%)	CLZ (%)	Silica content (%)
CLZ-MSPs	–	4.00 ± 0.22	96
DPPC—CLZ-MSPs	4.292 ± 0.037	2.99 ± 0.23	92.7
BL-DPPC—CLZ-MSPs (0.5 % BL in total lipid)	3.510 ± 0.004	3.38 ± 0.27	93.1

peak, indicative secondary phase transition due to the interaction of DPPC with BL. The main Tm of DPPC differs from the reported in literature, 41 °C (Campos Pacheco et al., 2025), which can be attributed to the different DSC measurement conditions between our study and the reported one, specifically the two different heating-cooling rates of 10 and 1.25 °C min^{-1}, respectively.

As particle morphology and coating quality can influence biological interaction, we relied on previously published data using the same MSPs batch and vesicle fusion method to infer physical characteristics. In that study (Campos Pacheco et al., 2025), SEM analysis showed that the uncoated MSPs were spherical with particles size of around 2.4 μm, and lipid coating via vesicle fusion yielded smooth, homogeneously coated particles without visible lipid aggregates. Given the identical MSPs batch and coating protocol used here, we expect comparable particle size and morphology in our novel formulations using bacterial lipids (BL). Additionally, we also proved that these coated particles via vesicle fusion could be effectively delivered to the lungs following a process of disaggregation in the lung fluid, further supporting distribution in the lung environment.

3.3. Study on the formation of foam macrophages

Since one of the biological targets in mycobacterial lung infections are the resistant mycobacteria internalized in macrophages, it is important to investigate the potential toxic effects of the lipid coated MSPs on macrophages. In particular, macrophages may over-uptake various lipid types and become foam cells afterwards (Yuan et al., 2012). The formation of foam cells stimulates macrophage activation, which can subsequently enhance the immune response through the release of inflammatory cytokines. Thereby, formation of the foam macrophages plays an important role in infection and directly affects the cells' functions. To study the effect of lipid coated MSPs, THP-1 human monocytes after differentiation (i.e., dTHP-1) were chosen since widely used as macrophage model for toxicity test in inhalation (Stueckle et al., 2024). Fig. 3 shows red lipid droplets indicating foam cell formation, as detected by Oil Red O staining. The images at lower magnification (20×) are also shown in Fig. S4 (supplementary information). Negative control showed the spontaneous formation of intracellular lipids in untreated cells, while cells treated with ox-LDL, were used as positive control of lipid-laden macrophages (Zhu et al., 2023). Visually, no fundamental differences were found after the incubation cells with empty MSPs and negative control, which suggests that formation of foam cells is completely absent after the presence of MSPs at the concentration tested. A slight propensity of lipid-laden macrophages was observed following incubation with DPPC-MSPs or bacterial lipids only. At the same time, a slight but well-defined response of dTHP-1 cells to incubation with BL-DPPC-MSPs was observed. It is noticeable that in the latter, dTHP-1 cells are morphologically transformed, elongated and acquire similarity to the positive control, as well as slightly stained lipid droplets are seen in the cytosol of most of cells. Therefore, it can be hypothesized that the BL-DPPC mixture lipid is solely responsible for weakly transforming dTHP-1 cells into foam cells. This weak reaction may indicate the formation of an immune response with the involvement of pro-inflammatory factors in response to the lipids burden of the cells. The effect of bacterial lipids on metabolism and polarization of human macrophages is a less-studied, complicated process with deep involvement of biological, immunological and molecular aspects, that needs a comprehensive and separate study (Teng et al., 2017).

3.4. Killing efficacy of extra- and intracellular mycobacteria via coating with bacterial lipids

DPPC-coated MSPs have been proven to drastically improve the release and dissolution rate of the encapsulated drug, clofazimine, an antitubercular drug, by enhancing its interaction with lung surfactant, mucus, and lung epithelial tissue (Campos Pacheco et al., 2025). Thus, this study investigates on whether phospholipid and bacterial lipid coatings affect the antimycobacterial activity of CLZ-encapsulated MSPs against mycobacteria. Fig. 4 shows the effect of bacterial lipids (BL) and DPPC coating on the antimicrobial activity of CLZ-MSPs against extra- and intra- cellular mycobacteria. In particular, Fig. 4A shows that BL-DPPC—CLZ-MSPs was more effective in inhibiting mycobacteria growth at intermediate drug concentrations (1.25 and 2.5 μg/mL)

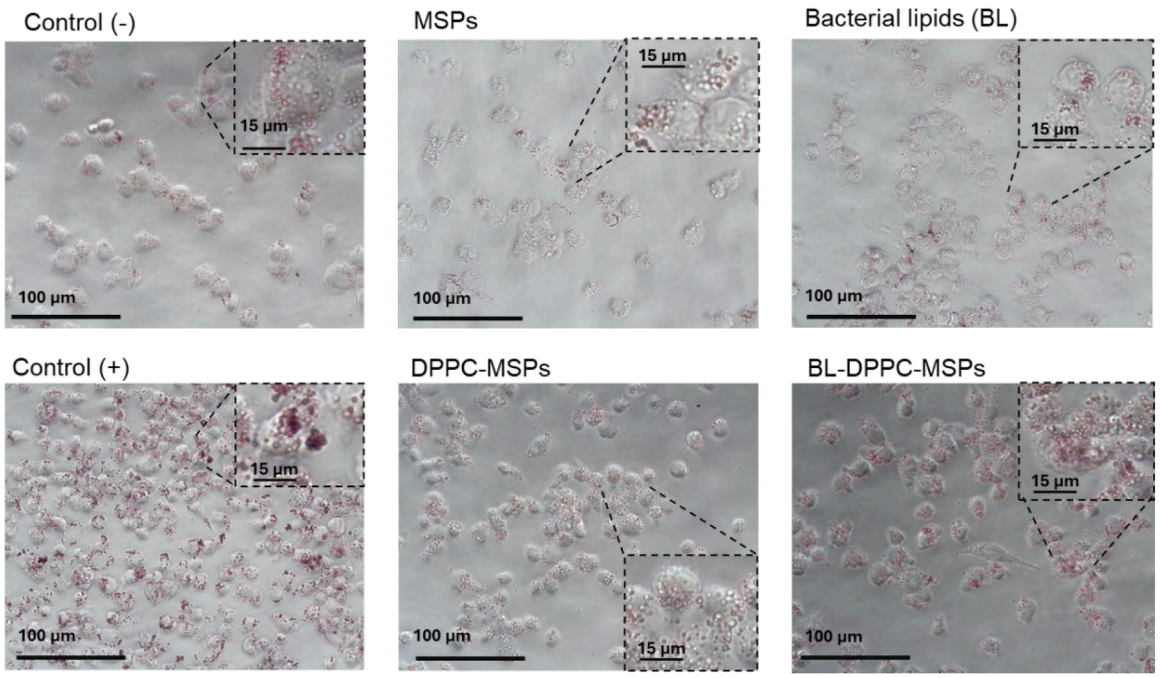

Fig. 3. Representative Oil Red O-stained light microscopy images of dTHP-1 macrophages treated with serum free RPMI medium (control -), 100 µg/mL ox-LDL (control +), 0.06 mg/mL uncoated MSPs (MSPs), 0.06 mg/mL DPPC-coated MSPs (DPPC-MSPs), 0.06 mg/mL bacterial lipid coated-DPPC-MSPs (BL-DPPC-MSPs) and 0.01 µg/mL bacterial lipids (BL) for 24 h. Images magnification: 40×. The zoom in images is highlighted inside the dotted line squares.

compared to uncoated CLZ-MSPs ($p = 0.004$ and 0.0065, respectively) and DPPC-coated CLZ-MSPs ($p = 0.0003$ and 0.0276, respectively). At 0.31 - 0.63 µg/mL CLZ dose, no significant difference was observed between BL and DPPC coating on CLZ-MSPs, but both systems exhibited greater activity compared to uncoated CLZ-MSPs ($p = 0.0298$ and <0.0001 for BL-coated, and $p = 0.0087$ and 0.006 for DPPC-coated CLZ-MSPs, respectively). In contrast, no significant difference was observed for all the MSPs formulations either at lower or higher doses of CLZ, in the ranges of 0.15 – 0.31 and 5 −10 µg/mL, respectively. Of interest, BL-DPPC—CLZ-MSPs at a concentration of 0.63 µg/mL was comparable or slightly more effective to inhibit the mycobacteria growth than rifampicin at 1 µg/mL, used as a positive control since it is a well-stablished first line anti-TB drug (Schön et al., 2009). The data was presented also as percentage of mycobacterial inhibition (%) in Fig. S5 (supplementary information). The overall effectiveness of BL and DPPC coating could be attributed to an increased drug dissolution kinetics, as reported in our previous work demonstrating that lipid coating exhibited an improved CLZ release from MSPs and dissolution kinetics in aqueous solution (Campos Pacheco et al., 2025). However, BL-DPPC—CLZ-MSPs' greater antimicrobial activity compared to DPPC—CLZ-MSPs at intermediate drug concentrations is likely due to an inherent effect of the BL coating. It has been reported that cardiolipin (CL) increased the antimicrobial activity of a new amphiphilic aminoglycoside derivative on *Pseudomonas aeruginosa*, by affecting the growth of bacteria (Swain et al., 2018). Nevertheless, the direct anti-mycobacterial effectiveness of the BL-containing particles is not known and needs further investigation.

From a therapeutic perspective in the lungs, killing the intracellular mycobacteria, that is hiding in human primary macrophages is essential. Deliver CLZ directly into the infected cells by MSPs is therefore a strategy for drug delivery. In this regard, Fig. 4B shows that the BL-DPPC—CLZ-MSPs were more effective on intracellular killing at low dose concentration of CLZ (i.e., from 0.16 to 0.31 µg/mL) ($p < 0.0001$ compared to DPPC—CLZ-MSPs and CLZ-MSPs), which could be attributed to the composition of the bacterial lipid mixture/cocktail as discussed above. For CLZ concentrations equal and above 0.31 µg/mL, incorporating bacterial lipids into the lipid coating of CLZ-MSPs does not improve intracellular antimicrobial effect compared to DPPC coated CLZ-MSPs; however, both DPPC coated and BL-DPPC uncoated CLZ-MSPs exhibit a higher killing effect than uncoated CLZ-MSPs up to 1.25 µg/mL. The lack of effectiveness above this concentration can be related to solubility limitations and saturation of CLZ inside the infected cells. Rifampicin, at therapeutic concentration (1 µg/mL) (Schön et al., 2009), was used as a control, showing that encapsulated antibiotics maintains a similar intracellular mycobacterial killing (Tenland et al., 2019). These results could be further attributed to our previous finding that lipid coating exhibited an improved CLZ release from MSPs and dissolution kinetics in aqueous solutions (Campos Pacheco et al., 2025). To summarize, our data indicated that the incorporation of bacterial lipids increases the killing effect of both extra and intracellular mycobacteria in infected macrophages.

Additionally, to evaluate the potential efficacy of using the novel drug delivery system for CLZ to combat TB, it must be demonstrated that this loaded system can not only kill pulmonary bacteria but also disseminated mycobacteria. Therefore, this dry powder formulation was tested against BCG after serum inoculation, for potential intravenous TB treatment. The results (Fig. 4C) shows that BL-DPPC-MSPs preserves CLZ during serum incubation. A dose response of CLZ in coated MSPs was observed in mycobacteria inhibition (%) from 42 % to 78 % in the concentration range of 0.15 −0.63 µg/mL, and this mycobacteria inhibition remained stable up to 10 µg/mL. The BL-DPPC-MSPs were shown to preserve the effective form of CLZ also after 2 and 3 h of serum incubation. In contrast, under serum-free conditions, the inhibition was notably less pronounced, suggesting that the incubation with serum may ensure drug release. These findings support the idea that the formulation retains the active form of CLZ in systemic circulation, highlighting its potential to target bacteria at extrapulmonary sites via the bloodstream.

Our findings extend the scope of lipid-based coatings for mesoporous silica particles (MSPs) by introducing a bacterial lipid (BL) and DPPC that combines the biophysical advantages of both surfactant and bacterial lipids. Previous work using *M. smegmatis*–derived lipid reconstituted nanoparticles (LrNs) has largely focused on mycolic-acid–rich membrane components to drive antimicrobial synergy and proinflammatory signaling (Pu et al., 2024). In contrast, our BCG lipid

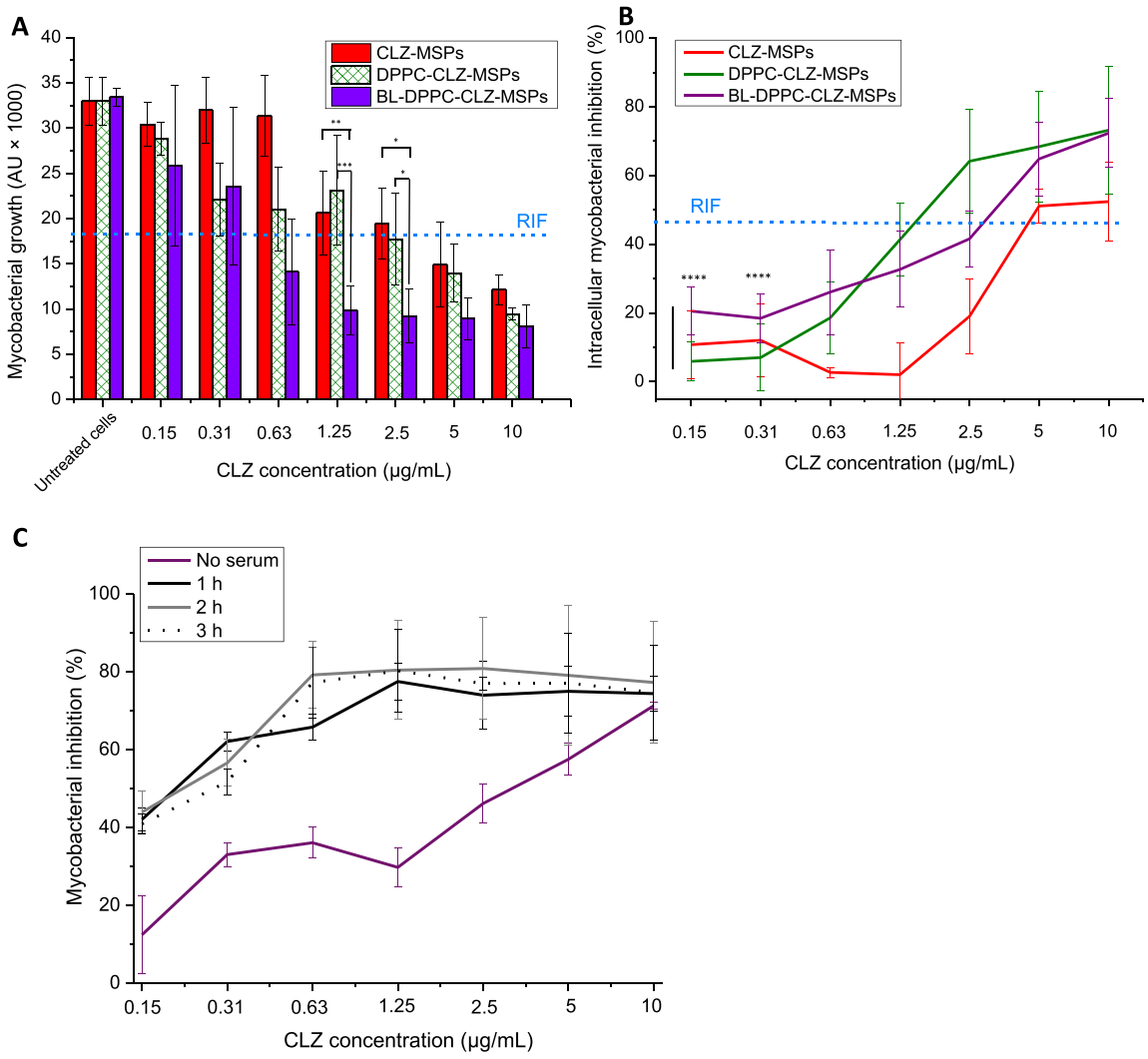

Fig. 4. **A**) Minimum inhibitory concentration (MIC) for CLZ, DPPC—CLZ-MSPs and BL-DPPC—CLZ-MSPs. Rifampicin (1 μg/mL) and untreated BCG were used as controls. **B**) Intracellular MIC for CLZ, DPPC—CLZ-MSPs and BL-DPPC—CLZ-MSPs after incubation (1 week). Rifampicin (RIF, 1 μg/mL) and untreated infected macrophages were used as controls. **C**) Mycobacterial inhibition (%) for BL-DPPC—CLZ-MSPs after 1, 2, 3 h incubation in human serum, mimicking the intravenous treatment of dissiminated TB. Data without serum is also included as comparison. Results are based on three biologically independent experiments ($n = 3$). Two-way ANOVA was used to analyse differences in mycobacterial growth and inhibition across formulations and concentrations. Statistical significance is indicated as follows: $^{*}p < 0.05$, $^{**}p < 0.005$, $^{***}p < 0.001$, $^{****}p < 0.0001$.

fraction is dominated by phospholipid species (cardiolipin, phosphatidylcholine, and phosphatidylethanolamine) that maintain vesicle fusion and promote intracellular delivery.

As a result, clofazimine-loaded, BL–DPPC–coated MSPs achieve superior intracellular mycobacterial killing in primary human macrophages and THP-1 cells at low drug concentrations (0.16 - 0.31 μg/mL), compared to DPPC coating only or uncoated MSPs. Notably, this increased efficacy occurs without compromising mitochondrial activity or inducing foam cell formation, in contrast to the potent proinflammatory responses observed with *M. smegmatis* bacterial lipid liposomes (Mishra et al., 2023).

To understand the involvement of immunoregulatory effects after treatment with CLZ loaded in BL-DPPC-MSPs, the release of TNFα and CCL2 was evaluated as a dose response from human primary macrophages. TNFα is a key proinflammatory cytokine, known to be crucial for both protective immunity and immunopathology during *M. tuberculosis* infection (Yuk et al., 2024). Produced mainly by lung macrophages in early *M. tuberculosis* infection, it is also essential for granuloma formation, preventing chronic infection, and recruiting and activating macrophages at the infection site. The cytokine CCL2, on the other hand, is essential for the influx of inflammatory monocytes, which can further differentiate into resident tissue macrophages during TB (Peters et al., 2001). The results (see supplementary information, Table S1 and S2) demonstrated that the levels of TNFα and CCL2 were similar to the cytokine concentration for RIF at the same concentration. Fig. S6 (supplementary information) shows the regression line used for quantification of cytokines based on the optical density absorbance. This implies that BL-DPPC-MSPs loaded with CLZ could modulate the immune response, reflected in this study as decreased cytokine production.

To reveal more about the impact of the extracted bacterial lipids on human macrophages, we investigated the mitochondrial activity of M1-like (proinflammatory, mediating resistance to pathogens) and M2-like (anti-inflammatory, promoting tissue modeling) macrophages. Using the MTT assay, we assessed mitochondrial activity after 24 h of incubation with BL at a concentration of 0.5 mg/mL (Fig. 5A). Our findings showed an improvement in the mitochondrial activity of both M1-like and M2-like macrophages, revealing a good biocompatibility for the BL extract at the investigated concentration (0.5 mg/mL). This data are in agreement with our previous studies (Rocío Hernández et al., 2024; Campos Pacheco et al., 2024) that consistently showed no measurable

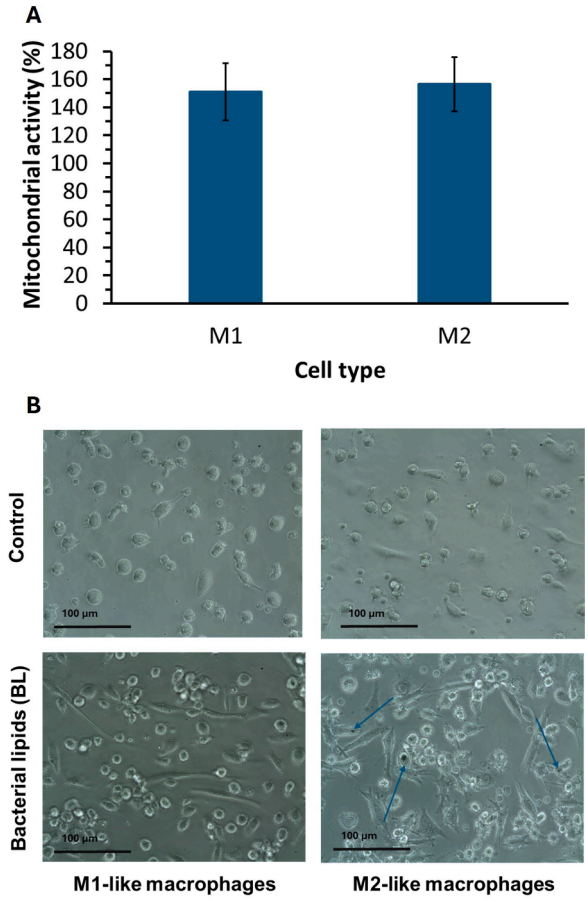

Fig. 5. **A**) The mitochondrial activity of M1-like and M2-like macrophages after 24 h incubation with bacterial lipids (BL, 0.5 mg/mL). The mitochondrial activity was assessed using the MTT assay. Data are presented as the mean percentage of mitochondrial activity normalized to untreated cells ± SD from three independent experiments (n = 5 for each experiment). **B**) Light microscopy images of morphological changes in M1-like and M2-like macrophages cells after 24 h incubation with bacterial lipids (0.5 mg/mL). Untreated macrophages are visualized as controls. Cells morphology changed from a rounded shape to elongated. Blue arrows indicated intracellular dark "inclusions" inside M2 cells, which could be attributed to accumulated bacterial lipids.

toxicity on either macrophages or Calu-3 cells across a broad concentration range of MSPs (7.8 µg/mL to 1 mg/mL), nor any impairment of epithelial integrity.

In Fig. 5B, morphological changes of primary macrophages after 24 h incubation with the bacterial lipids compared to untreated cells are shown. Moreover, presence of some single inclusions in M2-like macrophages, possibly may be lipid drops, which, combined with the highly changed shape of the cells, resemble foam macrophages, in agreement with the images with dTHP-1 macrophage-like cells (Fig. 3). Fig. S8 (supplementary information) shows the optical image at lower magnification. Altogether, the findings might suggest that the BL extracts from BCG could potentially influence macrophage polarization. Other in vitro studies confirm the transformation of macrophages from M1 to M2 phenotype following infection with *M. tuberculosis* (Vassiliou and Farias-Pereira, 2023; Huang et al., 2015). This correlates with the opinion that *M. tuberculosis* can change the metabolism of M2 cells in the direction of lipid accumulation to support the intracellular bacterial survival (Shim et al., 2020). However, polarised M2 macrophages are also able to suppress tuberculous granuloma formation (Huang et al., 2015), which could be an additional beneficial effect of BL-DPPC—CLZ-MSPs.

Due to numerous related factors, distinguishing macrophage subtypes during in vitro bacterial lipid exposure is challenging, as their phenotypes and functions vary. The environment influences cell polarization in each case. Further studies, using quantitative flow cytometry analysis, are needed to confirm this hypothesis and explore the mechanisms in detail.

4. Conclusions

This study successfully demonstrated the potential of coating mesoporous silica particles with bacterial lipids extracted from Mycobacteria toward a more efficient antimicrobial drug carrier. The lipid profiling revealed a complex mixture of lipids from BCG, including cardiolipin, which were effectively deposited on mesoporous silica particles (MSPs) via vesicle fusion. The cytotoxicity study showed enhanced mitochondrial activity in M1-like and M2-like macrophages indicating good biocompatibility. The antimicrobial activity tests indicated that, by including bacterial lipids in the formulation of lipid coated and loaded MSPs with clofazimine, the drug exhibited slightly greater activity inhibiting mycobacteria and killing intracellular mycobacteria compared to uncoated and DPPC-coated CLZ-MSPs. These findings further support the suitability of lipid coated-MSPs for enhancing drug dissolution, intracellular uptake, and overall biological efficacy compared to the free drug. Our results highlight the potential of bacterial lipid coatings as an alternative system for drug delivery and for treating mycobacterial infections, offering a promising strategy for combat lung infections with the current limitations of antibiotic resistance.

CRediT authorship contribution statement

Jesús E. Campos Pacheco: Writing – review & editing, Writing – original draft, Visualization, Validation, Methodology, Investigation, Formal analysis. **Camilla Davids:** Writing – review & editing, Writing – original draft, Validation, Methodology, Investigation, Formal analysis. **Tetiana Yalovenko:** Writing – review & editing, Writing – original draft, Validation, Methodology, Investigation, Formal analysis. **Elin Näsström:** Writing – review & editing, Validation, Methodology, Investigation. **Maria Ahnlund:** Writing – review & editing, Methodology, Investigation. **Gabriela Godaly:** Writing – review & editing, Writing – original draft, Validation, Supervision, Methodology, Investigation, Conceptualization. **Sabrina Valetti:** Writing – review & editing, Writing – original draft, Supervision, Project administration, Methodology, Funding acquisition, Formal analysis, Conceptualization.

Acknowledgments

This research was funded by the Swedish Research Council (Vetenskapsrådet) grant 2019–05163 and by the Knowledge Foundation (KK-stiftelsen) grant 20190101. The authors gratefully acknowledge Dr. Komal Rao-Fransson for her support during the culturing and harvesting of *M. bovis*.

Supplementary materials

Supplementary material associated with this article can be found, in the online version, at doi:10.1016/j.ejps.2025.107225.

Data availability

Data will be made available on request.

References

Boiten, W., et al., 2016. Quantitative analysis of ceramides using a novel lipidomics approach with three dimensional response modelling. Biochimica et Biophysica Acta (BBA) - Molecular Cell Biol. Lipids 1861 (11), 1652–1661.

Campos Pacheco, J.E., et al., 2024. Inhalable porous particles as dual micro-nano carriers demonstrating efficient lung drug delivery for treatment of tuberculosis. J. Control Release 369, 231–250.
Campos Pacheco, J.E., et al., 2025. Bioinspired lipid coated porous particle as inhalable carrier with pulmonary surfactant adhesion and mucus penetration. J. Colloid. Interface Sci. 697, 137967.
Chunfang Zhou, A.F., Paszkiewicz, Paulina, 2018. Xin Xia A Process for Manufacturing Porous Silica Particles Loaded with at Least One Bioactive Compound Adapted for Lung, Nasal, Sublingual and/or Pharyngeal Delivery. E.P. Office, Editor.
Diab, J., et al., 2019. Lipidomics in ulcerative colitis reveal alteration in mucosal lipid composition associated with the disease State. Inflamm. Bowel. Dis. 25 (11), 1780–1787.
Ferreras, J.A., et al., 2008. Mycobacterial phenolic glycolipid virulence factor biosynthesis: mechanism and small-molecule inhibition of polyketide chain initiation. Chem. Biol. 15 (1), 51–61.
Hiraishi, Y., et al., 2011. Bacillus Calmette-Guérin vaccination using a microneedle patch. Vaccine 29 (14), 2626–2636.
Huang, Z., et al., 2015. Mycobacterium tuberculosis-induced polarization of Human macrophage orchestrates the formation and development of tuberculous granulomas In vitro. PLoS. One 10 (6), e0129744.
Jiang, C., Gamarnik, A., Tripp, C.P., 2005. Identification of lipid aggregate structures on TiO2 surface using headgroup IR bands. J. Phys. Chem. B 109 (10), 4539–4544.
Mamaeva, V., Sahlgren, C., Linden, M., 2013. Mesoporous silica nanoparticles in medicine–recent advances. Adv. Drug Deliv. Rev. 65 (5), 689–702.
Matteelli, A., et al., 2025. Update on multidrug-resistant tuberculosis preventive therapy toward the global tuberculosis elimination. Int. J. Infect. Diseases 155.
Migliori, G.B., et al., 2025. Post Tuberculosis Lung Disease: questions and answers. Eur. Respirat. J., 2500992
Mishra, M., et al., 2023. Mycobacterial lipid-derived immunomodulatory drug- liposome conjugate eradicates endosome-localized mycobacteria. J. Controlled Release 360, 578–590.
Onwueme, K.C., et al., 2005. The dimycocerosate ester polyketide virulence factors of mycobacteria. Prog. Lipid Res. 44 (5), 259–302.
Peters, W., et al., 2001. Chemokine receptor 2 serves an early and essential role in resistance to mycobacterium tuberculosis. Proc. Natl. Acad. Sci. u S. a 98 (14), 7958–7963.
Pirson, C., et al., 2012. Differential effects of Mycobacterium bovis - derived polar and apolar lipid fractions on bovine innate immune cells. Vet. Res. 43 (1), 54.
Pu, X., et al., 2024. Lipids extracted from mycobacterial membrane and enveloped PLGA nanoparticles for encapsulating antibacterial drugs elicit synergistic antimicrobial response against mycobacteria. Mol. Pharm. 21 (5), 2238–2249.
Rao, K.U., et al., 2021. A broad spectrum anti-bacterial peptide with an adjunct potential for tuberculosis chemotherapy. Sci. Rep. 11 (1), 4201.
Reynolds, M.B., Abuaita, B.H., O'Riordan, M.X., 2020. Cardiolipin dynamics regulate proinflammatory cytokine production in methicillin-resistant Staphylococcus aureus–infected macrophages. J. Immunol. 204 (1_Supplement), p. 152.14-152.14.
Rocío Hernández, A., et al., 2024. Disordered mesoporous silica particles: an emerging platform to deliver proteins to the lungs. Drug. Deliv. 31 (1), 2381340.
Schön, T., et al., 2009. Evaluation of wild-type MIC distributions as a tool for determination of clinical breakpoints for mycobacterium tuberculosis. J. Antimicrob. Chemother 64 (4), 786–793.
Seung, K.J., Keshavjee, S., Rich, M.L., 2015. Multidrug-resistant tuberculosis and extensively drug-resistant tuberculosis. Cold. Spring. Harb. Perspect. Med. 5 (9), a017863.
Shim, D., Kim, H., Shin, S.J., 2020. Mycobacterium tuberculosis infection-driven foamy macrophages and their implications in tuberculosis control as targets for host-directed therapy. Front. Immunol. 11.
Stueckle, T.A., et al., 2024. In vitro inflammation and toxicity assessment of pre- and post-incinerated organomodified nanoclays to macrophages using high-throughput screening approaches. Part Fibre Toxicol. 21 (1), 16.
Swain, J., et al., 2018. Effect of cardiolipin on the antimicrobial activity of a new amphiphilic aminoglycoside derivative on Pseudomonas aeruginosa. PLoS. One 13 (8), e0201752.
Teng, O., Ang, C.K.E., Guan, X.L., 2017. Macrophage-bacteria interactions-A lipid-centric relationship. Front. Immunol. 8, 1836.
Tenland, E., et al., 2018. A novel derivative of the fungal antimicrobial peptide plectasin is active against mycobacterium tuberculosis. Tuberculosis. (Edinb) 113, 231–238.
Tenland, E., et al., 2019. Effective delivery of the anti-mycobacterial peptide NZX in mesoporous silica nanoparticles. PLoS. One 14 (2), e0212858.
Vassiliou, E., Farias-Pereira, R., 2023. Impact of lipid metabolism on macrophage polarization: implications for inflammation and tumor immunity. Int. J. Mol. Sci. 24 (15), 12032.
Vergnolle, O., et al., 2015. Biosynthesis of cell envelope-associated phenolic glycolipids in Mycobacterium marinum. J. Bacteriol. 197 (6), 1040–1050.
Wauthoz, N., Amighi, K., 2014. Phospholipids in pulmonary drug delivery. Eur. J. Lipid Sci. Technol. 116 (9), 1114–1128.
WHO, World Tuberculosis Day 2025. 2025.
Yalovenko, T., Campos Pacheco, J.E., Sedelius, G., Schousboe, E., Alionte, A., Pilkington, G., Gustafsson, A., Valetti, S., Mesoporous Silica Particles as Dual Micro-Nano Carriers for Pulmonary Therapy: Assessing Macrophage Safety, submitted, 2025.
Yuan, Y., Li, P., Ye, J., 2012. Lipid homeostasis and the formation of macrophage-derived foam cells in atherosclerosis. Protein Cell 3 (3), 173–181.
Yuk, J.M., et al., 2024. TNF in Human tuberculosis: a double-edged sword. Immune Netw. 24 (1), e4.
Zhu, C., et al., 2023. TRIM64 promotes ox-LDL-induced foam cell formation, pyroptosis, and inflammation in THP-1-derived macrophages by activating a feedback loop with NF-κb via iκbα ubiquitination. Cell Biol. Toxicol. 39 (3), 607–620.